

The cost of quantum yield

John R. Swierk*

Department of Chemistry, State University of New York at Binghamton, Vestal, NY USA 13850

KEYWORDS Quantum yield, photoredox, photochemical reactor, radical chain

ABSTRACT: The quantum yield of a photocatalytic reaction significantly influences its performance, as reactions with low quantum yields require more intense light sources and longer illumination times to achieve efficient reaction rates. Unfortunately, the importance of quantum yield is often overlooked in the design of photocatalytic reactions for small molecule synthesis, leading to potential cost implications and reduced productivity. This study examines various photochemical reactor designs from the literature to estimate photon flux and light generation costs, and investigates the impact of quantum yield on both cost and productivity. The findings reveal substantial penalties in cost and productivity when quantum yields are low. For instance, external quantum yields below 1% can result in significant light generation costs and maximum productivities of less than one mole of product per day. Moreover, the study highlights that high quantum yields have a larger effect on potential productivity than high product yields. By optimizing for quantum yield instead of product yield, kinetic and revenue modeling for the photoredox-mediated synthesis of ceralasertib demonstrate the potential for generating hundreds of thousands of dollars in additional revenue per day. Overall, this work emphasizes the need for increased consideration of quantum yield in the design of photocatalytic reactions.

Over the last ten plus years, the recognition of light as a tool within synthetic chemistry has enabled the development of new and transformative methods for small molecule synthesis.¹⁻⁴ Light is harvested by a photocatalyst, which can then be transferred to a substrate via energy transfer or the photon's energy can be converted into an electrical potential and used to drive electron transfer between the excited photocatalyst and a substrate. The later class of reactions, termed photoredox, generate radical species that then undergo non-photochemical (i.e., dark) reaction steps to generate the final product. Unlike many traditional synthetic methods, photochemical reactions typically occur at or near room temperature, with the energy needed to surmount the reaction barrier provided by a photon, though reactions that incorporate a second catalytic cycle (e.g., dual photoredox) sometimes exhibit enhanced performance at higher temperatures.⁵ Consequently, the energy input from light should be considered alongside other raw material inputs in terms of utilization and cost within a reaction.

In principle, the energy input for a photochemical reaction could come from directly solar power, which is both sustainable and free (neglecting system manufacturing and cooling costs) and solar reactors capable of kg-scale manufacturing have been demonstrated.⁶ However, direct use of solar energy for large-scale photochemical manufacturing also presents challenges such as low photon fluxes, intermittency, and broadband illumination including UV light. Some photocatalytic reactions exhibit wavelength-dependent chemoselectivity, which can result impact the product distribution.⁷ Photoinduced decomposition or transformation of the active catalytic species also poses a challenge in the design and utilization of some reactions.^{8,9} Some of these challenges can be overcome with reactor design (e.g., the use of concentrating reactors) but that can introduce new challenges such intense heat generation and the need for efficient cooling. Instead, the majority of large-scale

photoreactors have relied on artificial light sources (e.g., LEDs).¹⁰ While the electricity for these light sources could be generated from solar sources, issues of intermittency still exist and generally grid electricity is used. In addition, lack of data about reactor design, reaction mechanisms, and the temporal performance of a reaction have all served to limit the development of new reactions and reactors.¹¹

The use of light within a photochemical reaction can be assessed with different metrics. Energy intensity is a metric widely adopted within green chemistry and is defined as the total process energy divided by the mass of the final product.^{12,13} The Bunsen-Roscoe law states that the photochemical effect of a reaction is directly proportional to the energy dose regardless of the illumination time (intensity of light x illumination time = constant).¹⁴ This in turn relates to the inverse-square law of light, which describes the decrease in light intensity with increasing distance from the light source. These laws highlight the relationship between light intensity and kinetics, which in turn relate to the reaction quantum yield (QY). The reaction QY can be defined as either the internal QY (moles of product produced/moles of photons absorbed) or external QY (moles of product produced/moles of incident photons). Due to the widespread use of the term "quantum yield" in the literature, that term is used in this discussion. However, it is important to note that the term photonic yield or apparent yield may also be used instead of external QY and is recommended by IUPAC to distinguish from the term "quantum yield," which in this case would be analogous to internal QY.¹⁵ In addition, the use of "efficiency" is recommended when dealing with broadband illumination, while "yield" is recommended for monochromatic light sources. In general, the discussion in this manuscript explicitly or implicitly assumes monochromatic illumination and so the term "quantum yield" is used.

A low internal QY indicates kinetic inefficiency within the reaction with one or more unproductive pathways outcompeting the desired, productive pathway (e.g., inefficient excited state quenching). The external QY incorporates information about the internal QY as well as light losses related to scattering, incomplete light harvesting, and light loss due to reactor design. Thus, a low external QY could be related to a low internal QY or to some aspect of reaction or reactor design. Unfortunately, despite the prevalence of accessible methods to measure QY,¹⁶⁻²¹ the QY of synthetic electron transfer and photoredox reactions is not widely reported and measurement of QY is not a standard characterization metric for new reports.

Within a photochemical reaction, the QY predominantly impacts the rate of the reaction, with a low QY leading to slow product generation. Use of more intense light sources can increase the rate of product formation,²² however in some cases increasing the light intensity can lead to a change in mechanism and decrease in QY.²³ Understanding the interplay between QY, reaction rate, and cost is critical to enable the development of large-scale photochemical syntheses and to shape the development of new photochemical methods. Unfortunately, there is a gap in our understanding of how QY impacts the viability of a reaction, particularly at scale. The analysis reported here narrows that gap by presenting the first detailed estimation of the cost of QY in both real dollars and lost productivity. Using data from experimentally demonstrated photoreactors, both the photon flux and light generation costs per mole of photons can be estimated. Low external QY can to introduce meaningful costs for light generation and hard limits on possible reactor productivity. From an economic productivity standpoint, optimization of QY the below analysis suggests that optimizing reactions for QY is more beneficial than optimizing for product yield (PY). In all cases, radical chain reactions, where more than one product molecule is generated from a single photon, are shown to be desirable from both a cost and productivity standpoint. Overall, this work highlights the need for increased studies of the relationship between QY, reaction mechanism, and reactor design.

RESULTS AND DISCUSSION

Analysis of photoreactors. As a starting point for understanding the impact of QY, we can begin by estimating the photon flux and cost per mole of photons for different photochemical reactors.²⁴⁻³⁶ The photon flux was estimated based on the total optical power within the system and makes no assumptions about distance from the light source. For entries 1, 3, 4, and 7, the optical power within the reactor was measured directly. For all other entries, the optical power was estimated based on the reported optical power of the light source. It is important to note that photon fluxes in Table 1 represent the optimal photon flux, however the photon flux will decrease over time and thus decrease reactor productivity, though that is not considered in these estimates.

The cost per mole of photons was estimated using a modification of the method described by Sender and Ziegenbalg.³⁷ Specifically, the cost was estimated using the electricity cost for each light source, the cost of replacing each light source pro-rated over estimated lifetime, and electricity costs associated with cooling (see supporting information for complete details). Costs associated with the fabrication of reactor, purchase and replacement of a power supply, and purchase of cooling system (e.g., a chiller) were not included and instead treated as upfront

system costs, which were not considered in this analysis. There are also other limitations in these estimates that should be acknowledged. A cost of \$0.073 per kWh of electricity was assumed based on the US national average for industrial electricity in January 2022,³⁸ though the cost of electricity can vary widely based on location. The lifetime of the light source also introduces significant uncertainty. Many of the lifetimes are based on estimates, which may vary significantly depending on a variety of environmental factors (e.g., efficiency of cooling, duty cycle). Replacement costs are based on these estimated lifetimes of the light sources, which could be underestimated or overestimated. In addition, the cost of light source replacement could be decreased via economy of scale with large scale photoreactors. It is worth noting, however, that while ultraviolet and longer wavelength ($\lambda > 540$ nm) LEDs have significant room for improvement in power conversion efficacy, blue LEDs are currently approaching their theoretical maximum efficacy.³⁹ This suggests little potential for future increase photon fluxes for many of reactor designs described in Table 1. Finally, the costs of cooling are difficult to estimate as the degree of insulation and amount of heat generated by the light sources will have a significant impact on the chiller efficiency and power consumption.

Table 1: Photon flux, cost per mole of photons, and experimental productivity for various photoreactors

Entry	Reactor Type	Light Source	Wave-length (nm)	Photon Flux (mol photon/s)	Cost per mol photons (\$)	Moles of photons per day	Experimental Productivity (mol/day)	Estimated QY ^a	Ref.
1	Merck Batch Reactor	LED	450	6.89×10^{-6}	0.115	0.595	0.0011 – 0.422	0.002 – 0.709	24
2	3D-Printed Reactor	LED	440	1.79×10^{-4}	0.087	15.5	.0328	0.002	25
3	Merck Continuous Flow Reactor	LED	405	2.90×10^{-3}	0.076	251	46.5	0.186	26
4	Merck Plug Flow Reactor	LED	440	2.87×10^{-3}	0.0441	248	201.7	0.813	27
5	Corning Advanced Flow G3 Photo Reactor	LED	405	1.85×10^{-3}	0.092	160	410.3	2.567	28
6	Falling Film Reactor	LED	395	4.95×10^{-6}	0.054	0.428	0.0356	0.083	29
7	Continuous Flow Reactor	Medium Pressure Hg Lamp	200-300	8.30×10^{-5}	1.972	7.17	0.87	0.121	30
8	Parallel Quartz Tube Reactor	Low Pressure Hg Lamp	254	1.02×10^{-4}	0.091	8.81	0.023	0.003	31
9	Laser-Based Continuous Stirred Tank	CW Laser	450	2.45×10^{-4}	0.7994	21.2	204.5	9.661	32
10	Continuous Stirred-Tank Reactor	LED	440	2.68×10^{-4b}	0.0553	23.2	0.0104	4.49×10^{-4}	33
11	Vapourtec E UV-150	LED	450	9.04×10^{-5}	0.2425	7.81	0.007	0.001	34
12	Bristol Meyers Squib Large-Scale Flow Photoreactor	LED	395	2.73×10^{-3}	0.086	236	20.0	0.085	35
13	Pacer Photo-chemistry Illuminator	LED	525	4.85×10^{-5}	1.66	4.18	0.707	0.169	36

^aQY for the reactor estimated by dividing experimental productivity by photon flux per day^bSee Supporting Information for discussion of photon flux

Table 1 shows the estimated photon flux and cost per mole of photons for 13 notable examples of photoreactors described in the literature. While the list is not comprehensive, most common photoreactor architectures are represented.¹⁰ There is a wide range in estimated photon flux from 4.95×10^{-6} mol photons/s to 2.9×10^{-3} mol photons/s. In the case of LED-based systems, the difference in photon flux is overwhelmingly driven by a difference in the number of LEDs. The estimated costs per mole of photons are generally on the order of less the \$0.10, with the exception of the entries 7, 9, 11, and 13. In these cases, the increase cost per mole of photons driven largely by large replacement costs for the light sources (Figure S1). The cost estimates in Table 1 are in good agreement with Sender and

Ziegenbalg,³⁷ especially when accounting differences in electricity costs. Also, the electrical efficiencies for most of the high-power LEDs used in the photoreactors analyzed for this study are somewhat lower than the ~0.4 to 0.5 in the Sender and Ziegenbalg estimates. Finally, Table 1 also includes the experimental productivity reported for each photoreactor. Care must be taken in the comparison of the productivity data since each data point is on different reactions with different OY.

Generally, as the flux of the reactor increases, the experimental productivity also increases. There is not a strong correlation between cost per mole of photon and photon flux, with the highest photon flux (entry 3) having an estimated cost per mole of photon of \$0.076. Interestingly, the entries with the highest experimental productivity (entries 5 and 9) produce

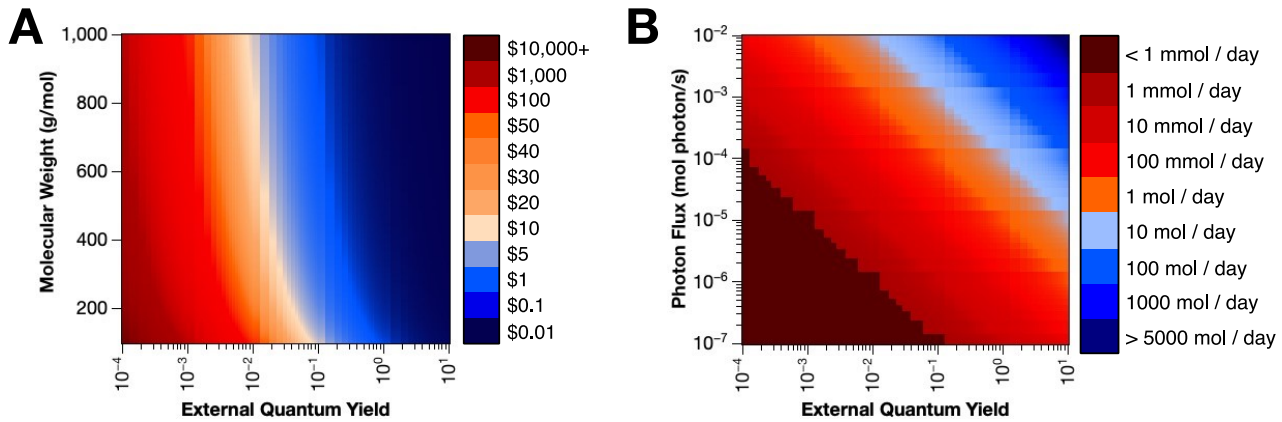


Figure 1. A) Added cost of light generation as a function of external QY and product molecule weight, assuming a cost per mole of photons of \$0.08. B) Maximum productivity per day as a function of external quantum yield and photon flux.

significantly more moles of product than predicted by the theoretical light output of the reactor. This strongly suggests radical chain behavior. Entry 9, a photoredox trifluoromethylation, proceeds via a radical chain where an iodine radical propagates the reaction.³² Entry 5 also likely proceeds via a radical chain, as bromination reactions are known to exhibit radical chain behavior.^{40,41} The rest of the experimentally demonstrated productivities utilize less than 100% of the predicted photon flux. Only entries 1 and 4 convert a moderate to large fraction of reagents into products (0.709 and 0.813, respectively). The rest of the entries in Table 1 convert less than 20% of the photons produced by the reactor into product.

The ratio of the experimental productivity to the estimated photon flux essentially estimates the external QY for the reaction in Table 1. Low values likely arise from a combination of a low QY for the target reaction and reactor design. For example, in a flow reactor light may be lost by scattering off tubing or in illuminating portions of the reactor without tubing. Having a photocatalyst concentration too low to absorb nearly all incoming photons could represent another light loss pathway. Any reactor where light from the illumination source can be seen outside of the reactor is exhibiting light loss that limit the external QY to below 1 for any non-chain reactions.

Economic and productivity impact of quantum yield. QY primarily relates to the rate of the reaction; a low QY typically results in a reaction that is slow to reach completion. The impact of QY on the reaction can manifest in one of two ways. Either QY can introduce increased costs due to light generation or through an opportunity cost related to lower productivity.

Figure 1A shows the cost per kilogram of product as a function of external QY and molecular weight. The light cost per kilogram is calculated using a cost per mole of photons of \$0.08, which is within the reasonable range for a highly productive photoreactor. Figure 1A shows that as the external QY of the reaction decreases below 1, the costs associated with light generation begin to increase. At an external QY of 0.1 and a product molecular weight (MW) of 200 g/mol, the costs associated with light generation are estimated to be \$4/kg. When the external QY goes lower, the added costs increase sharply to hundreds or thousands of dollars per kg of product. Figure 1A also shows that reactions with external QY greater than 1 (i.e., radical chain reactions) will have negligible costs associated with light generation. In radical chain reactions, an initial radical species is

generated and then generates additional radical species, which propagate the reaction. For a photoredox reaction, this means that one photon can generate multiple product molecules. While radical chain reactions are known to occur in photoredox catalysis,¹⁶ chain behavior is usually discovered after developing the reaction and is not an intentionally designed feature. Depending on reactor design, the data in Figure 1A suggests that an increased emphasis on the design and understanding of photoredox radical chain reactions may prove to be an interesting route to more efficient reactions. An example of this was demonstrated by Bonfield et al.⁴² who demonstrated that the radical chain Wohl-Ziegler reaction actually proceeds better with decreased light intensity and therefore lower power consumption.

In many cases, the added cost due to light generation is unlikely to have a significant impact on pharmaceutical synthesis, however, it is noteworthy that the low estimated QY for entries 10 and 11 introduce added light generation costs of \$668 and \$897 per kilogram of product, respectively. Also, the potential costs due to light generation could be significant in the synthesis of agrochemicals, which are significantly more sensitive to process costs.^{43,44}

In addition to increased costs due to light generation, a low QY introduces a separate opportunity cost that can be significant (see below) should also be considered. Figure 1B shows potential productivity per day as function of external QY and reactor photon flux. Based on the data in Table 1, the highest photon fluxes reported to date are approximately 2.9×10^{-3} moles of photons per second. At that photon flux, a reaction with an external QY of 1 could produce a maximum of 256 mol of product per day. Those numbers are in excellent good agreement with the experimental productivity of the Merck Plug Flow Reactor (Table 1, Entry 4). However, even at high photon fluxes, reactions with lower external QYs will struggle to generate even 10 mol of product per day. A stark contrast can be drawn to reactions with external QY of 1 or less and radical chain photoredox reactions. Even at low photon flux (1×10^{-4} mol photon/s), modest radical chain reactions are predicted to have productivities of 10 moles of product per day or greater. At a photon flux of 2×10^{-3} mol photon/s, a reaction with an external QY of 10 is predicted to generate 1728 moles of product per day. Entries 5 and 9 in Table 1 also demonstrate the potential impact of radical chain reactions on overall reactor productivity.

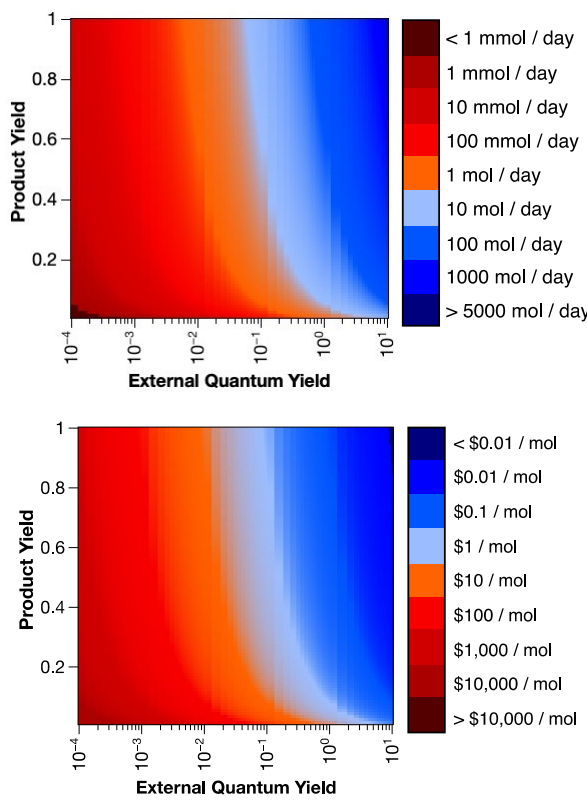


Figure 2. (top) Productivity per day as a function of PY and external quantum yield assuming a photon flux of 2×10^{-3} mol photon/s. (bottom) Additional light costs as a function of PY and external quantum yield assuming a photon flux of 2×10^{-3} mol photon/s and cost of \$0.08 per mole of photons.

In general, extremely low QY are not an unrealistic possibility as reports of QY on the order of 0.01 or less are common in the literature.⁴⁵⁻⁴⁸ We also recently demonstrated that experimental quencher concentrations for short-lived, organic photocatalysts are often much too low to ensure efficient quenching and therefore will lead to low QY.⁴⁹ It is also important to emphasize that the QY in Figure 1 is an external QY. Our recent work on the coupling of 1,4-dicyanobenzene and N-phenylpyrrolidine showed that while the internal QY of the reaction was close to 1 at early times, because of parasitic light absorption and scattering losses, the external QY was 0.3 or less.²² Similarly, a reactor design that does not ensure complete light absorption will also decrease the external QY.

Ideally, both the PY and QY of the reaction will be high. However, during the development of a new photoredox method, the PY of a reaction is usually the key focus for optimization, though that may not be the optimal strategy when considered through the lens of QY. The top panel of Figure 2 shows the daily productivity as a function of PY and external QY, while the bottom panel shows the added light cost as a function of PY and external QY, assuming a photon flux of 2×10^{-3} mol photon/s and a cost of \$0.08 per mole photon. At a PY and external QY of 1, 173 mol of product can be produced in a given day. However, when the external QY falls below 0.6, less than 100 mol of product will be produced per day. Realistically, complete conversion of all starting material and recovery of all product is often challenging or impossible, making practical PYs less than 1. As an example, a reaction with a product and external QY of 0.75 will produce less than 100 moles of product per day at a

light flux of 2×10^{-3} mol photon/s. In contrast, a reaction with a PY of 0.2 and an external QY of 10 will produce ~350 moles of product per day. While this analysis neglects other considerations such as product purification, it highlights that in some cases optimization of QY may be more productive than optimization of PY. In terms of added light generation costs, these costs only become significant in the context of pharmaceutical synthesis in the case of extremely low PY (<0.1) and low external QY (<0.001). For reactions that are more sensitive to economic considerations, Figure 2 shows that light generation costs depend most strongly on external QY.

Case study on the impact of QY. To explore the impact of QY on a real reaction, the photoredox-mediated synthesis of ceralasertib was examined. Ceralasertib is a commercially available compound that is also a promising anti-cancer compound currently in clinical trials.^{50,51} Graham et al.⁵² demonstrated that a key intermediate, 2,4-Dichloro-6-[1-(methylsulfonyl)cyclopropyl]pyrimidine, could be prepared via a large-scale photoredox approach using a flow reactor. In addition, an industrial scale synthesis for the conversion of 2,4-Dichloro-6-[1-(methylsulfonyl)cyclopropyl]pyrimidine to ceralasertib⁵³ is also available. Together, this provides a plausible, complete route to a commercially available product that incorporated a photoredox step (Scheme S1). In addition, some kinetic and mechanistic data, as well as QY and PY, was available for the photoredox step.⁵² Thus, through a combination of kinetic and revenue modeling, the economic impact of QY on a reaction at scale can be approximated.

Using the proposed reaction mechanism and available kinetic data, a simple kinetic model was developed (Supporting Information). Because the kinetics and mechanism of the 2,4-Dichloro-6-[1-(methylsulfonyl)cyclopropyl]pyrimidine photoredox reaction have not been characterized in detail, several rate constants had to be assumed in the modeling (Scheme S2). The key steps in the reaction involve oxidative quenching by a redox active phthalimide ester, which fragments into a methylsulfonylcyclopropyl radical that is then captured by chloropyrimidine. The resulting radical is then oxidized by the oxidized

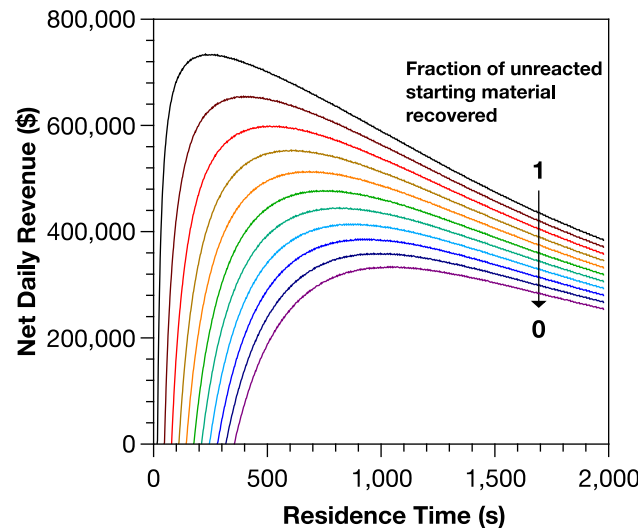


Figure 3. Predicted daily revenue based on material costs for the synthesis of ceralasertib as a function of residence time and recovered fraction of unreacted starting material going from complete recovery of unreacted material (1) to no recovery (0) in increments of 0.1.

photocatalyst to give 2,4-Dichloro-6-[1-(methylsulfanyl)cyclopropyl]pyrimidine. Several unproductive pathways not specified in the mechanistic were also added, including relaxation of the excited photocatalyst and oxidation of the methylsulfanyl-cyclopropyl radical by the oxidized photocatalyst. Most importantly, a decomposition step of the methylsulfanyl-cyclopropyl radical was included with a rate constant of $2.7 \times 10^8 \text{ s}^{-1}$. Inclusion of this step gave a PY of 52.5%, with 3.4% of the starting dioxoisindolin-2-yl)1-methylsulfanyl-cyclopropane-carboxylate left unreacted, both of which are in nearly identical agreement with the experimental report.⁵² The modeling predicts an initial QY of 0.33 that decays to 0.15 over 33 minutes. The initial QY is somewhat lower than the reported value (0.61), however, it is important to note that the experimental QY was determined based on consumption of the starting material and not on product generation. If the QY from the kinetic modeling data is calculated based on starting material consumption, a QY of 0.58 is obtained. Taken together, this demonstrates that the kinetic modeling reproduces the observed performance of the reaction quite well.

By using the PY and QY data obtained from the kinetic modeling, we can examine the influence of QY on the potential revenue generated from a raw material cost perspective in the synthesis of ceralasertib. Based on the published route to ceralasertib and raw material costs, the estimated total cost per gram of ceralasertib is \$4170 with a commercial price of \$14,700 (supporting information). For the revenue modeling, however, the cost was split into the cost associated with generating the product from the photochemical step, 2,4-Dichloro-6-[1-(methylsulfanyl)cyclopropyl]pyrimidine (\$2927.60 per gram), and then the cost associated with the subsequent transformation of the photochemical product. It is essential to note that this analysis focuses solely on raw material costs and does not include personnel and other operating expenses. Also, while the analysis considers the reported raw material costs associated with reagents for purification, the analysis does not consider personnel costs, reagents without specified amounts, or other costs connected with purification. However, despite these limitations, this approximation offers valuable insights into the impact of QY. It is also worth noting that 1 g of 2,4-Dichloro-6-[1-(methylsulfanyl)cyclopropyl]pyrimidine represents 0.00448 mol, meaning that 1 mol of 2,4-Dichloro-6-[1-(methylsulfanyl)cyclopropyl]pyrimidine would cost approximately \$653,282 to make. For the light generation costs to exceed 5% of the material costs, the PY would need to be less than 3% and the external QY would be less 0.0002. While the costs associated with different photochemical reactions obviously differ, this highlights how little the light generation costs can impact the final costs for a typical photochemical synthesis.

Figure 3 depicts the predicted daily revenue as a function of residence time and the fraction of unreacted starting material recovered. All curves exhibit a similar overall shape. Initially, at short residence times, a net negative revenue (not shown) is observed due to the relatively low PY compared to the daily volume of reagent consumed. For all the curves, the maximum PY of 52.5% is achieved at a residence time of 1980 s. However, the point of maximum revenue occurs prior to that time and is heavily dependent on the fraction of unreacted starting material that can be recovered. If complete recovery of unreacted starting material is achieved, the peak revenue is attained at a residence time of 228 s with a PY of only 12.3%. Conversely, in the absence of any unreacted starting material recovery, the peak revenue is reached at 1040 s with a PY of 41.9%.

Notably, the analysis consistently demonstrates that achieving the maximum PY does not correspond to the highest predicted revenue. This discrepancy arises from the decline in QY over time, resulting in a reduced rate of product formation during periods when photons are administered to the reaction, but minimal product is generated. Throughout a single day, the disparity between peak revenue and the revenue generated from the maximum PY can be substantial, ranging from over \$350,000 for complete starting material recovery to over \$80,000 for no starting material recovery. Extrapolated over a year, these differences amount to tens or hundreds of millions of dollars.

The primary limitation affecting the QY in the photoredox synthesis of 2,4-Dichloro-6-[1-(methylsulfanyl)cyclopropyl]pyrimidine is the incomplete quenching of the photocatalyst's excited state. According to data from Graham et al.,⁵² only approximately 58% of the excited states of 3DPA2FBN are quenched by (1,3-dioxoisindolin-2-yl)1-methylsulfanyl-cyclopropane-carboxylate (3DPA2FBN). This is primarily due to the short-lived excited state lifetime of 3DPA2FBN, which is 4.2 ns, making it inefficient for quenching through bi-molecular, diffusional interactions. By keeping all other kinetic parameters constant and using a photocatalyst with a slightly longer lifetime of 10 ns, the initial QY can be increased to 47%, resulting in a PY of 73.4% at a residence time of 1980 s. The increase in QY is driven by a higher percentage of quenched excited states (~82%). Photocatalysts with lifetimes around 10 ns are commonly found among organic photocatalysts, and transition metal and some organic photocatalysts can offer lifetimes exceeding 1 μs .^{54,55} On the other hand, the kinetic modeling can also be performed using a photocatalyst having a 1 ns lifetime. In this case, although the reaction achieves nearly the same PY (51%), a longer residence time of 2800 s is required to achieve max PY due to the significantly lower QY (initial QY of 16.5%). The decrease in QY and the corresponding increase in reaction time can be attributed to the inefficient utilization of excited states, as only 31% of them are quenched when using a photocatalyst with a 1 ns lifetime.

The impact of photocatalyst lifetime, and consequently the QY, on the net daily revenue can be observed in Figure 4. The figure displays the predicted net daily revenue for reactions with photocatalyst lifetimes of 1 ns, 4.2 ns, and 10 ns, assuming 30% of the unreacted starting material is recovered. Under these conditions, the peak revenue for the 1 ns photocatalyst is projected to be \$208,005 per day. However, with a longer lifetime of 4.2 ns, the peak revenue more than doubles, reaching \$414,767 per day. Despite both photocatalysts achieving nearly identical maximum PY, the higher QY associated with the 4.2 ns photocatalyst makes the reaction significantly more productive. Furthermore, at a lifetime of 10 ns, the maximum revenue reaches \$755,780 per day, even with only a modest increase in maximum PY.

While the preceding discussion focused on 2,4-Dichloro-6-[1-(methylsulfanyl)cyclopropyl]pyrimidine and ceralasertib, the findings are applicable to all photochemical reactions, as the QY tends to decrease as the reaction progresses toward completion. This decrease in QY can be attributed to various factors. One simple reason is that as the reaction proceeds, the rates of certain steps in the reaction slow down as different reagents are consumed. For instance, as the quencher is consumed during the reaction, the rate of quenching will decrease as the product conversion increases. Consequently, relaxation of the photocatalyst excited state can become competitive with quenching, leading

to a decrease in the internal QY. Additionally, byproducts generated during the reaction can also contribute to the decrease in QY. For example, in the coupling of 1,4-dicyanobenzene and N-phenylpyrrolidine, the production of acetic acid as a byproduct acts as a quencher in the reaction.²² Running a reaction to complete conversion will always be less productive than running a reaction to partial conversion while maintaining a high external QY. This suggestion is supported by the work of Lévesque et al., who demonstrated an almost four-fold improvement in overall productivity when they decreased residence time and reduced the conversion from maximum of 90% to 42%.²⁷

CONCLUSIONS

While QY has historically been neglected in the development and description of photoredox reactions, the above analysis demonstrates the significant financial and opportunity cost that a low QY imparts on a reaction. As a result, it is clear that developing reactions and reactors that give high external QYs may play a major role in the future development of industrially scalable photoredox chemistry. Recent reports demonstrate simple, approachable methods for measuring QY, which should enable the reporting of QY measurements as a standard practice in the disclosure of new photoredox reactions. Along with an increased focus on QY measurements, an increased mechanistic and kinetic understanding of photoredox reactions will be necessary to design new strategies to maximize QY. A recent perspective from Ziegenbalg et al. highlighted the importance of increased mechanistic and kinetic considerations and suggested a minimum set of reported parameters, including QY information, for reporting photochemical data.⁵⁶

Furthermore, the balance between PY and QY is important for optimizing photochemical reactions. While PY is typically the focus during reaction optimization, optimizing QY may lead to higher productivity. The above analysis demonstrates that reactions with lower external QYs struggle to generate significant product quantities, even at high photon fluxes. It is also clear from the above analysis that in some cases it may be better to optimize for QY instead of PY. In particular, low PY reactions with high QY may prove to be more economically viable than reactions with high PYs and inefficient light utilization. The case study of the photoredox-mediated synthesis of ceralasertib further supports the importance of QY in determining the potential revenue generated a synthetic process. While the analysis cannot completely capture all costs associated with the preparation of ceralasertib (e.g., personnel and purification costs), at a minimum it highlights that the impact of QY should be a consideration in the implementation of large-scale photochemical reactions.

In addition to a broader understanding of QY, this work highlights the opportunity to develop radical chain photoredox reactions. In terms of both light generation costs and overall productivity, reactions with a QY greater than 1 offer the promise of high productivity reactions. While many transformations may not amenable to a chain approach, the design principles for photoredox radical chain reactions and thus the potential scope are not well understood. In depth studies of known photoredox radical chain reactions may help enable the intentional development of further radical chain reactions.

Finally, this work emphasizes the need to further characterize and develop large-scale photoreactor designs. While the above

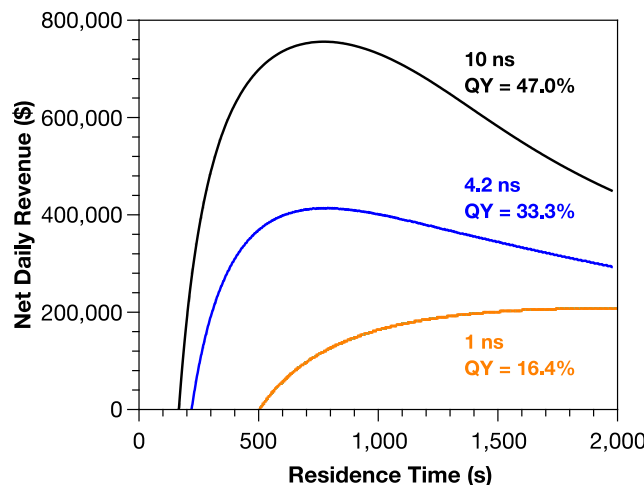


Figure 4. Predicted daily revenue based on material costs for the synthesis of ceralasertib as a function of residence time and photocatalyst lifetime: 10 ns (black curve), 4.2 ns (blue curve), and 1 ns (orange curve). Initial QY are reported for each curve. The analysis assumes that 30% of unreacted starting material is recovered.

analysis suggests that added light costs associated with light generation are likely not significant, more in-depth experimental studies are needed to confirm this. Experimental determination of photon fluxes and cooling requirements are necessary for more accurate analyses of cost and productivity impacts. Knowledge of the total photon flux within the reactor would also allow determination of external QY for large-scale reactors, which would help identify differences in internal versus external QY within the photoreactor and should lead to improvements in reactor design. Finally, studies focusing on long-term photoreactor operation are needed to understand whether estimated LED lifetimes bear out in operational conditions.

METHODS

The cost per mole of photons was estimated by considering the electricity cost for running the light source, the cost of replacing the light source(s) divided by the estimated lifetime of the light source, and the electricity cost associated with cooling the system. Replacement costs for the cooling system were not included except in the case of entry 2, which uses Peltier coolers with a known lifetime. A cost of \$0.073 per kWh of electricity was used in all calculations.³⁸ This was the average cost of electricity for industrial use across the United States in January 2022, though state by state costs vary widely from \$0.186 to 0.0532 within the contiguous United States. The lifetime of the different light sources was either taken from the manufacturer reports or, if unavailable, from the estimates used by Sender and Ziegenbalg.³⁷

If available, experimentally determined photon fluxes were reported in Table 1. Alternatively, specifications from the light source manufacturer were used to determine photon flux. The total photon flux was calculated and not normalized to area so that no assumptions about the distance of the light source from the reaction were made.

Complete details for all calculations are available in the supporting information.

Kinetic modeling. A complete description and discussion of the Kinetic modeling is available in the supporting information. In brief, using the mechanism and kinetic information provided

by Graham et al.,⁵² the reaction was rebuilt using Kinetoscope.⁵⁷ Where experimental rate constants were available, those values were used, otherwise plausible values for rate constants were assumed. Unproductive steps were also included, specifically relaxation of the excited photocatalyst, oxidation of the methyl-sulfanyl-cyclopropyl radical, and decomposition of the methyl-sulfanyl-cyclopropyl radical. The QY and PY of the reaction was particularly sensitive to the later step. Scheme S2 shows the complete assumed reaction mechanism and rate constants for the kinetic modeling.

Revenue modeling. A complete description and discussion of the revenue modeling is available in the supporting information. Using a photoredox-mediated route to cerasertib,^{52,53} the raw material costs associated with each step were determined using the lowest commercially-available price per gram or per liter. Using the QY and PY data available from kinetic modeling, the daily productivity and daily cost for the photochemical production of 2,4-Dichloro-6-[1-(methylsulfanyl)cyclopropyl]pyrimidine as a function of residence time was determined. A reported overall yield of 34.8% was used to calculate the conversion of 2,4-Dichloro-6-[1-(methylsulfanyl)cyclopropyl]pyrimidine to cerasertib. The costs associated with the conversion of 2,4-Dichloro-6-[1-(methylsulfanyl)cyclopropyl]pyrimidine were also determined and added to the costs for the synthesis of 2,4-Dichloro-6-[1-(methylsulfanyl)cyclopropyl]pyrimidine to give an overall cost for the synthesis of cerasertib. Varying fractions of unreacted starting material were assumed and the value of the recovered starting material was calculated using a value of \$743.95 per gram (see Table S2). The value of the cerasertib was determined by multiplying the daily predicted amount of cerasertib produced by the commercial price of \$14,7000 per gram.⁵⁸ To determine the net daily revenue, the estimated costs associated with producing cerasertib were subtracted from the value of the cerasertib and value of recovered starting material.

ASSOCIATED CONTENT

Supporting Information

The Supporting Information is available free of charge on the ACS Publications website.

Detailed calculations for the data in Table 1; percentage breakdown for total light costs for data in Table 1; details of kinetic modeling; predicted product and quantum yields from kinetic modeling; details of revenue modeling; raw material cost calculations for synthesis of cerasertib,(PDF)

AUTHOR INFORMATION

Corresponding Author

* jswierk@binghamton.edu

Funding Sources

NSF CHE-2047492

ACKNOWLEDGMENT

This work was supported by the National Science Foundation (NSF CHE-2047492). The author also thanks Filipa Siopa, Thomas Rehm, Melda Sezen-Edmonds, and Barney Mitchell for providing technical details related to different photoreactors.

REFERENCES

- Yoon, T. P.; Blum, T. R.; Skubi, K. L. Dual Catalysis Strategies in Photochemical Synthesis. *Chem. Rev.* **2016**, *116*, 10035–10074.
- Narayanan, J.M.R.; Stephenson, C.R.J. Visible Light Photoredox Catalysis: Applications in Organic Synthesis. *Chem. Soc. Rev.* **2011**, *40*, 102-113.
- Prier, C. K.; Rankic, D. A.; MacMillan, D. W. C. Visible Light Photoredox Catalysis with Transition Metal Complexes: Applications in Organic Synthesis. *Chem. Rev.* **2013**, *113*, 5322–5363.
- Romero, N. A.; Nicewicz, D. A. Organic Photoredox Catalysis. *Chem. Rev.* **2016**, *116*, 10075–10166.
- Candish, L.; Collins, K.D.; Cook, G.C.; Douglas, J.J.; Gómez-Suárez, A.; Jolit, A.; Kess, S. Photocatalysis in the Life Science Industry. *Chem. Rev.* **2022**, *122*, 2907-2980.
- Oelgemöller, M. Solar Photochemical Synthesis: From the Beginnings of Organic Photochemistry to Solar Manufacturing of Commodity Chemicals. *Chem. Rev.* **2016**, *116*, 9664-9682.
- Schmermund, L.; Reischauer, S.; Bierbaumer, S.; Winkler, C.K.; Diaz-Rodríguez, A.; Edwards, L.J.; Kara, S.; Mielke, T.; Cartwright, J.; Grogan, G.; Pieber, B.; Kroutil, W. Chemoslective Photocatalysis Enables Stereocomplementary Biocatalytic Pathways. *Angew. Chem. Int. Ed.* **2021**, *60*, 6965-6969.
- Gisbertz, S.; Reischauer, S.; Pieber, B. Overcoming Limitations in Dual Photoredox/Nickel Catalysed C-N Cross-Couplings Due to Catalyst Deactivation. *Nature Catal.* **2020**, *3*, 611-620.
- Devery III, J.J.; Douglas, J.J.; Nguyen, J.D.; Cole, K.P.; Flowers, R.A.; Stephenson, C.R.J. Ligand Functionalization as a Deactivation Pathway in *fac*-Ir(ppy)₃-mediated radical addition. *Chem. Sci.* **2015**, *6*, 537-541.
- Buglioni, L.; Raymenants, F.; Slattery, A.; Zondag, S.D.A.; Noël, T.A. Technological Innovations in Photochemistry for Organic Synthesis: Flow Chemistry, High-Throughput Experimentation, Scale-Up, and Photoelectrochemistry. *Chem. Rev.* **2022**, *122*, 2752-2906.
- Noël, T.; Zysman-Colman, E. The Promise and Pitfalls of Photocatalysis for Organic Synthesis. *Chem. Catal.* **2022**, *2*, 468-476.
- Sheldon, R.A. Metrics of Green Chemistry and Sustainability: Past, Present, and Future. *ACS Sustainable Chem. Eng.* **2018**, *6*, 32-48.
- Ruccolo, S.; Qin, Y.; Schindermann, C.; Nocera, D.G. General Strategy for Improving the Quantum Efficiency of Photoredox Hydroamination Catalysis. *J. Am. Chem. Soc.* **2018**, *140*, 14926-14937.
- Bonfield, H.E.; Knauber, T.; Lévesque, F.; Moschetta, E.G.; Susanne, F.; Edwards, L.J. Photons as a 21st Century Reagent. *Nature Comm.* **2020**, *11*, 804.
- Braslavsky, S.E.; Braun, A.M.; Cassano, A.E.; Emeline, A.V.; Litter, M.I.; Palmisano, L.; Parmon, V.N.; Serpone, N. Glossary of Terms Used in Photocatalysis and Radiation Catalysis (IUPAC Recommendations 2011). *Pure Appl. Chem.* **2011**, *83*, 931-1014.
- Cismesia, M.A.; Yoon, T.P. Characterizing Chain Processes in Visible Light Photoredox Catalysis. *Chem. Sci.* **2015**, *6*, 5426-5434.
- Pitre, S.P.; McTiernan, C.D.; Vine, W.; DiPucchio, R.; Grenier, M.; Sciano, J.C. Visible-Light Actinometry and Intermittent Illumination as Convenient Tools to Study Ru(bpy)₃Cl₂ Mediated Photoredox Transformations. *Sci. Rep.* **2015**, *5*, 16397.
- Roseau, M.; Chausset-Boissaire, L.; Gremetz, S.; Roth, P.M.C.; Penhoat, M. Multiple Wavelength (365–475 nm) Complete Actinometric Characterization of Corning® Lab Photo Reactor Using Azobenzene as a Highly Soluble, Cheap and Robust Chemical Actinometer. *Photochem. Photobiol. Sci.* **2022**, *21*, 421-432.
- Volfova, H.; Hu, Q.; Riedle, E. Determination of Reaction Quantum Yields: LED Based Setup with Better 5% Precision. *EPA Newsletter* **2019**, *96*, 51-69.
- Stadler, E.; Eibel, A.; Fast, D.; Freiheit, D.; Holly, C.; Wiech, M.; Moszner, N.; Gescheidt, G. A Versatile Method for the Determination of Photochemical Quantum Yields via Online UV-Vis Spectroscopy. *Photochem. Photobiol. Sci.* **2018**, *17*, 660-669.
- Buzzetti, L.; Crisenza, C.E.M.; Melchiorre, P. Mechanistic Studies in Photocatalysis. *Angew. Chem. Int. Ed.* **2019**, *58*, 3730-3747.
- Stevenson, B. G.; Spielvogel, E. H.; Loiaconi, E. A.; Wambua, V. M.; Nakhamiyayev, R. V.; Swierk, J. R.; Mechanistic Investigations of an α -Aminoarylation Photoredox Reaction. *J. Am. Chem. Soc.* **2021**, *143* (23), 8878-8885.
- Reiß, B.; Hu, Q.; Riedle, E.; Wagenknecht, H.-A. The Dependence of Chemical Quantum Yields of Visible Light Photoredox Catalysis on the Irradiation Power. *ChemPhotoChem* **2021**, *5*, 1009-1019.
- Le, C.; Wismer, M.K.; Shi, Z.-C.; Zhang, R.; Conway, D.V.; Li, G.; Vachal, P.; Davies, I.W.; MacMillan, D.W.C. A General Small-Scale Reactor to Enable Standardization and Acceleration of Photocatalytic Reactions. *ACS Cent. Sci.* **2017**, *3*, 647-653.
- Schiel, F.; Peinsipp, C.; Kornigg, S.; Böse, D. A 3D-Printed Open Access Photoreactor Designed for Versatile Applications in Photoredox-and Photoelectrochemical Synthesis. *ChemPhotoChem* **2021**, *5*, 431-437.
- Corcoran, E.B.; McMullen, J.P.; Lévesque, F.; Wismer, M.K.; Naber, J.R. Photon Equivalents as a Parameter for Scaling Photoredox Reactions in Flow: Translation of Photocatalytic C–N Cross-Coupling from Lab Scale to Multikilogram Scale. *Angew. Chem. Int. Ed.* **2020**, *59*, 11964-11968.
- Lévesque, F.; Di Maso, M.; Narsimhan, K.; Wismer, M.K.; Naber, J.R. Design of Kilogram Scale, Plug Flow Photoreactor Enabled by High Power LEDs. *Org. Process Res. Dev.* **2020**, *24*, 2935-2940.
- Steiner, A.; Roth, P.M.C.; Strauss, F.J.; Gauron, G.; Tekautz, G.; Winter, M.; Williams, J.D.; Kappe, C.O. Multikilogram per Hour Continuous Photochemical Benzylic Brominations Applying a Smart Dimensioning Scale-up Strategy. *Org. Process Res. Dev.* **2020**, *24*, 2208-2216.
- Fabry, D.C.; Ho, Y.A.; Zapf, R.; Tremel, W.; Panthöfer, M.; Rueping, M.; Rehm, T.H. Blue Light Mediated C–H Arylation of Heteroarenes using TiO₂ as an Immobilized Photocatalyst in a Continuous-Flow Microreactor. *Green Chem.* **2017**, *19*, 1911-1918.
- Hook, B.D.A.; Dohle, W.; Hirst, P.R.; Pickworth, M.; Berry, M.B.; Booker-Milburn, K.I.B. A Practical Flow Reactor for Continuous Organic Photochemistry. *J. Org. Chem.* **2005**, *70*, 7558-7564.
- Fortunato, M.A.G.; Ly, C.-P.; Siopa, F.; Afonso, C.A.M. Process Intensification for the Synthesis of 6-Allyl-6-azabicyclo[3.1.0]hex-3-en-2-ol from 1-Allylpyridinium Salt Using a Continuous UV-Light Photoflow Approach. *Methods Protoc.* **2019**, *2*, 67.
- Harper, K.C.; Zhang, E.-X.; Liu, Z.-Q.; Grieme, T.; Towne, T.B.; Mack, D.J.; Griffin, J.; Zheng, S.-Y.; Zhang, N.-N.; Gangula, S.; Yuan, J.-L.; Miller, R.; Huang, P.-Z.; Gage, J.; Diwan, M.; Ku, Y.-Y. Commercial-Scale Visible Light Trifluoromethylation of 2-Chlorothiophenol Using CF₃I Gas. *Org. Process Res. Dev.* **2022**, *26*, 404-412.
- Pomberger, A.; Mo, Y.; Nandiwal, K.Y.; Schultz, V.L.; Duvadie, R.; Robinson, R.J.; Atinoglu, E.I.; Jensen, K.F. A Continuous Stirred-Tank Reactor (CSTR) Cascade for Handling Solid-Containing Photochemical Reactions. *Org. Process Res. Dev.* **2019**, *23*, 2699-2706.
- DeLano, T.J.; Bandarage, U.K.; Palaychuk, N.; Green, J.; Boyd, M.J. Application of the Photoredox Coupling of Trifluoroborates and Aryl Bromides to Analgo Generation Using Continuous Flow. *J. Org. Chem.* **2016**, *81*, 12525-12531.
- Sezen-Edmonds, M.; Tabora, J.E.; Cohen, B.M.; Zaretsky, S.; Simmons, E.M.; Sherwood, T.C.; Ramierz, A. Predicting Performance of Photochemical Transformations for Scaling Up in Different Platforms by Combining High-Throughput Experimentation with Computational Modeling. *Org. Process Res. Dev.* **2020**, *24*, 2128-2138.
- Bonfield, H. E.; Mercer, K.; Diaz-Rodriguez, A.; Cook, G. C.; McKay, B. S. J.; Slade, P.; Taylor, G. M.; Ooi, W. X.; Williams, J. D.; Roberts, J. P. M.; Murphy, J. A.; Schmermund, L.; Kroutil, W.; Mielke,

T.; Cartwright, J.; Grogan, G.; Edwards, L. J. The Right Light: De Novo Design of a Robust Modular Photochemical Reactor for Optimum Batch and Flow Chemistry. *ChemPhotoChem* **2020**, *4*, 45-51.

37. Sender, M.; Ziegenbalg, D. Light Sources for Photochemical Processes – Estimation of Technological Potentials. *Chem. Ing. Tech.* **2017**, *89*, 1159-1173.

38. U.S. Energy Information Administration. Electric Power Monthly. https://www.eia.gov/electricity/monthly/epm_table_grapher.php?t=epmt_5_6_a (Accessed April 21, 2022)

39. Schroeder, E.; Christopher, P. Chemical Production Using Light: Are Sustainable Photons Cheap Enough? *ACS Energy Lett.* **2022**, *7*, 880-884.

40. Krosley, K.W.; Gleicher, G.J. Benzylic bromination by bromotrichloromethane. Dependence of the identity of the chain-carrying radical(s) on the method of initiation. *J. Org. Chem.* **1990**, *55*, 4469-4472.

41. Tanko, J.M.; Blackert, J.F. Free-Radical Side-Chain Bromination of Alkylaromatics in Supercritical Carbon Dioxide. *Science* **1994**, *263*, 203-205.

42. Bonfield, H.E.; Williams, J.D.; Ooi, W.X.; Leach, S.G.; Kerr, W.J.; Edwards, L.J. A Detailed Study of Irradiation Requirements Towards and Efficient Photochemical Wohl-Ziegler Procedure in Flow. *ChemPhotoChem* **2018**, *2*, 938-944.

43. Turner, M.K. Pharmaceuticals from agriculture: manufacture or discovery. *Indust. Crop Prod.* **1993**, *1*, 125-131.

44. Lamberth, C.; Jeanmart, S.; Luksch, T.; Plant, A. Current Challenges and Trends in the Discovery of Agrochemicals. *Science* **2013**, *341*, 742-746.

45. Romero, N.A.; Nicewicz, D.A. Mechanistic Insight into the Photoredox Catalysis of Anti-Markovnikov Alkene Hydrofunctionalization Reactions. *J. Am. Chem. Soc.* **2014**, *136*, 17024-17035.

46. Burykina, J.V.; Kobelev, A.D.; Shalpakov, N.S.; Kostyukovich, A.Y.; Fakhruddinov, A.N.; König, B.; Ananikov, V.P. Intermolecular Photocatalytic Chemo-, Stereo-, and Regioselective Thiol–Yne–Ene Coupling Reaction. *Angew. Chem. Int. Ed.* **2022**, *61*, e202116888.

47. Cardinale, L.; Schmotz, M.-O. W.S.; Konev, M.O.; Jacobi von Wangelin, A. Photoredox-Catalyzed Synthesis of α -Amino Acid Amides by Imine Carbamoylation. *Org. Lett.* **2022**, *24*, 506-510.

48. Sayre, H.; Ripberger, H.H.; Odella, E.; Zieleniewska, A.; Heredia, D.A.; Rubmles, G.; Scholes, G.D.; Moore, T.A.; Moore, A.L.; Knowles, R.R. PCET-Based Ligand Limits Charge Recombination with an Ir(III) Photoredox Catalyst. *J. Am. Chem. Soc.* **2021**, *143*, 13034-13043.

49. Soto, X.; Swierk, J.R. Using Lifetime and Quenching Rate Constant to Determine Quencher Concentration. *ACS Omega* **2022**, *7*, 25532-25536.

50. Yap, T. A.; Krebs, M. G.; Postel-Vinay, S.; El-Khouiry, A.; Soria, J.-C.; Lopez, J.; Berges, A.; Cheung, S. Y. A.; Irurzun-Arana, I.; Goldwin, A.; Felicetti, B.; Jones, G. N.; Lau, A.; Frewer, P.; Pierce, A. J.; Clack, G.; Stephens, C.; Smith, S. A.; Dean, E.; Hollingsworth, S. J. "Ceralasertib (AZD6738), an Oral ATR Kinase Inhibitor, in Combination with Carboplatin in Patients with Advanced Solid Tumors: A Phase I Study." *Clin. Cancer Res.* **2021**, *27*, 5213-5224.

51. Foote, K. M.; Nissink, J. W. M.; McGuire, T.; Turner, P.; Guichard, S.; Yates, J. W. T.; Lau, A.; Blades, K.; Heathcote, D.; Odedra, R.; Wilkinson, G.; Wilson, Z.; Wood, C. M.; Jewsbury, P. J. Discovery and Characterization of AZD6738, a Potent Inhibitor of Ataxia Telangiectasia Mutated and Rad3 Related (ATR) Kinase with Application as an Anticancer Agent. *J. Med. Chem.* **2018**, *61*, 9889– 9907.

52. Graham, M.A.; Noonan, G.; Cherryman, J.H.; Douglas, J.J.; Gonzalez, M.; Jackson, L.V.; Leslie, K.; Liu, Z.-Q.; McKinney, D.; Munday, R.H.; Parson, C.D.; Whittaker, D.T.E.; Zhang, E.-x.; Zhang, J.-w. Development and Proof of Concept for a Large-Scale Photoredox Additive-Free Minisci Reaction. *Org. Process Res. Dev.* **2021**, *25*, 57-67.

53. Graham, M.A.; Askey, H.; Campbell, A.D.; Chan, L.; Cooper, K.G.; Cui, Z.; Dalgleish, A.; Dave, D.; Ensor, G.; Espinosa, M.R.G.; Hamilton, P.; Heffernan, C.; Jackson, L.V.; Jing, D.; Jones, M.F.; Liu, P.; Mulholland, K.R.; Pervez, M.; Popadyne, M.; Randle, E.; Tomasi, S.; Wang, S. Development and Scale-Up of an Improved Manufacturing Route to the ATR Inhibitor Ceralasertib. *Org. Process Res. Dev.* **2021**, *25*, 43-56.

54. Arias-Rotonda, D. M.; McCusker, J. K. The Photophysics of Photoredox Catalysis: A Roadmap for Catalyst Design. *Chem. Sci. Rev.* **2016**, *45*, 5803-5820.

55. Romero, N. A.; Nicewicz, D. A. Organic Photoredox Catalysis. *Chem. Rev.* **2016**, *116*, 10075–10166.

56. Ziegenbalg, D.; Pannwitz, A.; Rau, S.; Dietzek-Ivanšić, B.; Streb, C. Comparative Evaluation of Light-Driven Catalysis: A Framework for Standardized Reporting of Data. *Angew. Chem. Int. Ed.* **2022**, *61*, e202114106

57. W. D. Hinsberg and F. A. Houle, Kinetiscope, available at <http://www.hinsberg.net/kinetiscope>, accessed May 18, 2023.

58. <https://www.selleckchem.com/products/azd6738.html> (accessed August 18, 2022)

